

# NUMERICAL SIMULATION OF LEAKAGE FROM A GEOLOGIC DISPOSAL RESERVOIR FOR CO<sub>2</sub>, WITH TRANSITIONS BETWEEN SUPER- AND SUB-CRITICAL CONDITIONS

Karsten Pruess

Earth Sciences Division, Lawrence Berkeley National Laboratory, Berkeley, CA 94720  
e-mail: K\_Pruess@lbl.gov

## ABSTRACT

The critical point of CO<sub>2</sub> is at temperature and pressure conditions of  $T_{crit} = 31.04\text{ }^{\circ}\text{C}$ ,  $P_{crit} = 73.82\text{ bar}$ . At lower (subcritical) temperatures and/or pressures, CO<sub>2</sub> can exist in two different phases, a liquid and a gaseous state, as well as in two-phase mixtures of these states. Disposal of CO<sub>2</sub> into brine formations would be made at supercritical pressures. However, CO<sub>2</sub> escaping from the storage reservoir may migrate upwards towards regions with lower temperatures and pressures, where CO<sub>2</sub> would be in subcritical conditions. An assessment of the fate of leaking CO<sub>2</sub> requires a capability to model not only supercritical but also subcritical CO<sub>2</sub>, as well as phase changes between liquid and gaseous CO<sub>2</sub> in sub-critical conditions. We have developed a methodology for numerically simulating the behavior of water-CO<sub>2</sub> mixtures in permeable media under conditions that may include liquid, gaseous, and supercritical CO<sub>2</sub>. This has been applied to simulations of leakage from a deep storage reservoir in which a rising CO<sub>2</sub> plume undergoes transitions from supercritical to subcritical conditions. We find strong cooling effects when liquid CO<sub>2</sub> rises to elevations where it begins to boil and evolve a gaseous CO<sub>2</sub> phase. A three-phase zone forms (aqueous - liquid - gas), which over time becomes several hundred meters thick as decreasing temperatures permit liquid CO<sub>2</sub> to advance to shallower elevations. Fluid mobilities are reduced in the three-phase region from phase interference effects. This impedes CO<sub>2</sub> upflow, causes the plume to spread out laterally, and gives rise to dispersed CO<sub>2</sub> discharge at the land surface. Our simulations suggest that temperatures along a CO<sub>2</sub> leakage path may decline to levels low enough so that solid water ice and CO<sub>2</sub> hydrate phases may be formed.

## 1. INTRODUCTION

There is general consensus in the technical community that geologic disposal of CO<sub>2</sub> into saline aquifers would be made at supercritical pressures (Holloway and Savage, 1993; Hitchon et al., 1999). The critical point of CO<sub>2</sub> is at temperature and pressure conditions of  $T_{crit} = 31.04\text{ }^{\circ}\text{C}$ ,  $P_{crit} = 73.82\text{ bar}$  (Vargaftik, 1975). At lower (subcritical) temperatures and/or pressures, CO<sub>2</sub> can exist in two

different phases, a liquid and a gaseous state, as well as two-phase mixtures of these states (Fig. 1). Supercritical CO<sub>2</sub> forms a phase that is distinct from the aqueous phase, and can change continuously into either gaseous or liquid CO<sub>2</sub> with no phase boundaries. CO<sub>2</sub> leaking from a disposal reservoir could flow upward towards regions with lower temperatures and pressures, where CO<sub>2</sub> would be in subcritical conditions. An assessment of potential leakage behavior therefore requires a capability to model not only supercritical CO<sub>2</sub>, but also subcritical CO<sub>2</sub>, as well as phase changes between liquid and gaseous CO<sub>2</sub>. This paper introduces a methodology for numerically simulating the behavior of water-CO<sub>2</sub> mixtures in permeable media under conditions that may include all different phase compositions.

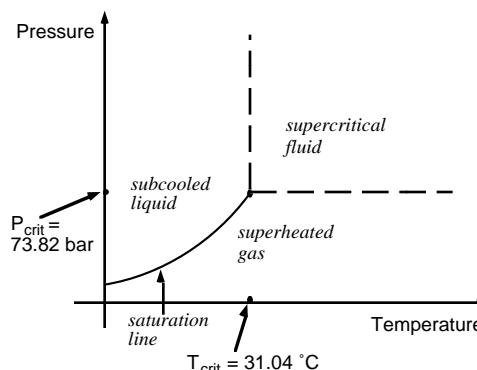


Figure 1. Phase states of CO<sub>2</sub>.

The thermodynamic issues relevant to upflow of CO<sub>2</sub> from a deep storage reservoir are illustrated in Fig. 2. The saturation pressure of CO<sub>2</sub> as a function of temperature is shown along with two hydrostatic pressure profiles, calculated for a typical geothermal gradient of 30 °C per km, for two average land surface temperatures of 5 °C and 15 °C, respectively. Both profiles pass in the vicinity of the critical point of CO<sub>2</sub>, and the one for 5 °C surface temperature intersects the CO<sub>2</sub> saturation line. This indicates that a bubble of CO<sub>2</sub> that is migrating upward would undergo a phase transition from liquid to gas at a pressure of approximately 63 bars, corresponding to a depth of approximately 630 m. Leakage of CO<sub>2</sub> from a deeper brine formation may cause some overpressure, which would shift the pressure profiles

towards higher values. Phase change from liquid to gas is to be expected if CO<sub>2</sub> escapes upward at rates large enough so that not all of the leaking CO<sub>2</sub> can be retained as dissolved solute in the aqueous phase.

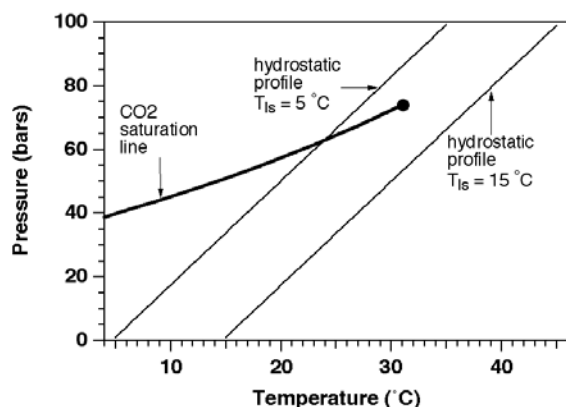


Figure 2. CO<sub>2</sub> saturation line and hydrostatic pressure-temperature profiles for typical continental crust. The saturation line ends at the critical point, here marked with a solid circle.

Phase change may have large effects on leakage rates, because CO<sub>2</sub> density is much lower for the gaseous than for the liquid state (Fig. 3). At subsurface (T, P) conditions, liquid CO<sub>2</sub> is always less dense than

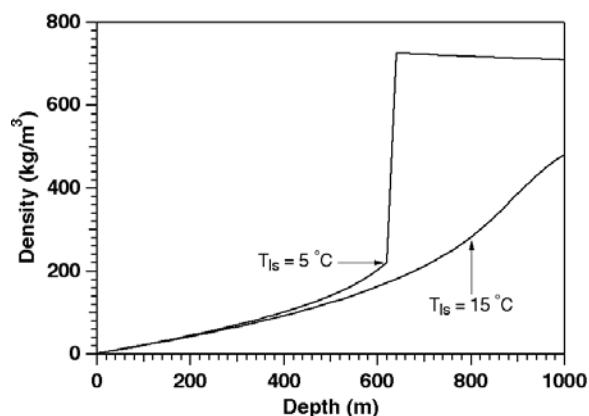


Figure 3. CO<sub>2</sub> density versus depth along the two hydrostatic profiles shown in Fig. 2.

aqueous phase and thus is subject to upward buoyancy force. A transition to gaseous conditions would greatly enhance the buoyancy forces and could accelerate fluid leakage, as well as causing a rapid increase in fluid pressures at shallower horizons. This in turn could open pre-existing faults and fractures, enhancing their permeability and further increasing leakage rates. Reduced CO<sub>2</sub> solubility at the lower fluid pressures prevailing at shallower depths would also come into play.

It is of interest to examine whether these processes and effects can be self-enhancing to the point where they could cause a catastrophic, eruptive failure of a CO<sub>2</sub> disposal system (Chivas et al., 1987). Catastrophic releases of CO<sub>2</sub>-rich gas with fatalities have occurred at two lakes in Cameroon, in 1984 at Lake Monoun (Sigurdsson et al., 1987), and in 1986 at nearby Lake Nyos (Tazieff, 1991). Pruess and García (2002) simulated the migration of CO<sub>2</sub> up a fault under supercritical conditions. Their simplified model showed some self-enhancement of CO<sub>2</sub> discharge rates, but only in a gradual, bounded manner.

This paper presents a first exploratory study of CO<sub>2</sub> leakage under conditions that involve phase transitions from liquid to gaseous CO<sub>2</sub>. We first summarize our treatment of fluid phase conditions, and then proceed to investigate CO<sub>2</sub> leakage behavior under conditions that involve an interplay of three fluid phases: a - aqueous, l - liquid CO<sub>2</sub>, and g - gaseous CO<sub>2</sub>.

## 2. FLUID PHASE CONDITIONS

The two-component system water-CO<sub>2</sub> may exist in any one of seven different phase combinations (Fig. 4): three single-phase states, three two-phase states, and a three-phase state. Modeling of this system needs

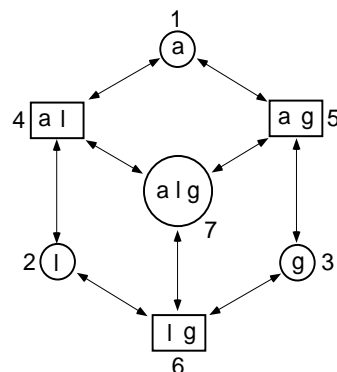


Figure 4. Possible phase combinations in the system water-CO<sub>2</sub>. The phase designations are a - aqueous, l - liquid CO<sub>2</sub>, g - gaseous CO<sub>2</sub>.

to address the following:

- accurate representation of thermophysical properties of water-CO<sub>2</sub> mixtures (density, viscosity, enthalpy, mutual solubility) in terms of appropriate sets of primary thermodynamic variables (such as temperature, pressure, mass fractions of components, phase saturations);
- recognition of phase conditions and phase change (appearance or disappearance).

The correlations of Altunin et al. (1975) are used in this paper to represent properties of CO<sub>2</sub> over a broad range of temperature and pressure conditions within experimental accuracy, except for narrow intervals around the critical point where larger errors occur. Water properties are likewise obtained within experimental accuracy from the steam table equations given by the International Formulation Committee (1967). Partitioning of water and CO<sub>2</sub> among different co-existing phases (mutual solubility) is calculated on the basis of local thermodynamic equilibrium, i.e., requiring chemical potentials of a component to be equal in different phases. Certain approximations are made in the actual implementation of the chemical equilibrium constraints (Pruess and García, 2002). Brines are modeled as NaCl solutions, with realistic dependence of density, viscosity, enthalpy, and vapor pressure of the aqueous phase on solute concentration (Battistelli et al., 1997). Effects of salinity on CO<sub>2</sub> solubility in the aqueous phase are described with an extended version of Henry's law (Pruess and García, 2002).

Within the context of numerical simulation of water-CO<sub>2</sub> mixtures, it is actually more convenient not to use the Altunin et al. (1975) correlations directly. Instead, we employ these correlations to generate CO<sub>2</sub> properties on a 2-D grid of temperature and pressure values, and then obtain parameters needed during the simulation by linear interpolation on this grid (Fig. 5). One advantage of this approach is that

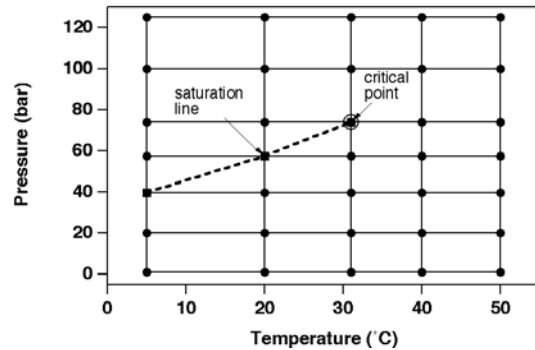


Figure 5. Schematic of the temperature-pressure tabulation of CO<sub>2</sub> properties.

table lookup and interpolation are computationally much faster than calculating the full correlations, while providing excellent accuracy for a modest number of table points (of order of 100 each in the temperature and pressure domains). Tabular data also facilitate easy recognition of all phase conditions for CO<sub>2</sub>. This is accomplished by including grid points on the saturation line itself in the tabulation (Fig. 5). More specifically, we specify a sequence of sub-critical temperatures, calculate their saturation pressures  $P_{\text{sat}}(T)$ , and include these temperatures and

pressures in the tabulation. The critical temperature and pressure are also included. Additional table points are generated for pressures lower than the smallest  $P_{\text{sat}}$ , for pressures larger than  $P_{\text{crit}}$ , and for temperatures larger than  $T_{\text{crit}}$ . Points on the saturation line have two sets of property data attached to them, one set for liquid and the other for gaseous CO<sub>2</sub>.

## 2.1 Numerical Treatment

Depending on fluid phase composition, different thermodynamic parameters may not be independent, and different sets of independent thermodynamic variables must be used. In most TOUGH2 modules, different phase compositions are distinguished by means of distinctive numerical ranges of the primary thermodynamic variables (Pruess et al., 1999). For systems with three or more active phases, however, it is more convenient to use a numerical index to distinguish different phase compositions (Adenekan et al., 1993; Pruess and Battistelli, 2002), and that is the approach adopted here.

Distinguishing phase compositions through indexing rather than through the numerical values of primary variables has certain advantages, such as allowing a finite window for phase appearance rather than using a “hair trigger” criterion. For example, in two-phase aqueous-gas conditions we need to determine whether a liquid phase can evolve to form a three-phase system. To do this we monitor CO<sub>2</sub> partial pressure,  $P_{\text{CO}_2} = P - P_{\text{sat},w}(T)$ , where  $P_{\text{sat},w}$  is the saturated vapor pressure of water. From a thermodynamic viewpoint, a liquid phase will evolve when  $P_{\text{CO}_2}$  exceeds saturated CO<sub>2</sub> pressure  $P_{\text{sat},\text{CO}_2}$ . However, our numerical experiments have shown that the criterion  $P_{\text{CO}_2} > P_{\text{sat},\text{CO}_2}$  for a transition to three-phase conditions may lead to very unstable behavior, where liquid phase may frequently appear and disappear during the iteration process, seriously limiting the progress of the flow simulation in time. By using a separate phase index it is possible to adopt a more robust criterion, where a liquid phase is evolved only when  $P_{\text{CO}_2}$  exceeds  $P_{\text{sat},\text{CO}_2}$  by a finite amount,  $P_{\text{CO}_2} > 1.001 \times P_{\text{sat},\text{CO}_2}$ , say. Strictly speaking, a state with  $P_{\text{CO}_2} > P_{\text{sat},\text{CO}_2}$  cannot exist in two-phase aqueous-gas conditions. However, allowing  $P_{\text{CO}_2}$  to slightly exceed  $P_{\text{sat},\text{CO}_2}$  without evolving liquid entails a small inaccuracy in the physical properties of CO<sub>2</sub>, with negligible impacts on longer-term simulation results, while greatly improving the efficiency of the simulation. As will be seen below, transitions from a-g to a-l-g conditions occur frequently when simulating upward migration of CO<sub>2</sub>. It is only through introduction of a finite albeit small phase change window that this process can be efficiently simulated.

More detailed discussion of thermophysical property treatment and phase transition handling is given in (Pruess and García, 2002; Pruess, 2003).

### 3. LEAKAGE SIMULATION

When supercritical CO<sub>2</sub> migrates upward from depth, its thermodynamic state will change towards lower pressures and temperatures, and a transition to sub-critical conditions may take place (Fig. 2). Eventually the liquid CO<sub>2</sub> will boil into gas, a process that involves significant heat transfer effects due to the latent heat of vaporization. The thermal effects make the process multi-dimensional even under idealized conditions where upflow would be confined to a vertical 1-D channel with impermeable boundaries. The simplest geometry in which the coupling between fluid flow and heat transfer can be modeled involves a two-dimensional radially symmetric (2-D R-Z) system, in which a permeable channel at the center may exchange heat with the surrounding rock. This is the geometric configuration adopted here for a first exploration of phase change effects during upward migration of CO<sub>2</sub>. In investigating this simplified system, our purpose is to bring out the main fluid and thermodynamic effects that determine the behavior of CO<sub>2</sub> discharge from a geologic disposal reservoir. Future work should aim at a more realistic description of potential CO<sub>2</sub> storage reservoirs, and geometric and hydrogeologic properties of potential pathways for CO<sub>2</sub> leaks (Hitchon et al., 1999).

#### 3.1 Model System

We consider a flow system in the shape of a cylinder with 1000 m vertical thickness (see Fig. 6). The outer boundary at a radius of 200 m is intended to be “far” from the main flow activity. A vertical channel of 3 m radius with a permeability of  $k = 10^{-13} \text{ m}^2$  is located at the center, while the surrounding medium is modeled as homogeneous and isotropic with a permeability of  $10^{-14} \text{ m}^2$ , a factor 10 smaller than the channel. Additional parameters include porosity  $\phi = 0.35$ , pore compressibility  $c = 4.5 \times 10^{-10} / \text{Pa}$ , thermal conductivity  $K = 2.51 \text{ W/m}^\circ\text{C}$ , specific heat of the rock  $c_R = 920 \text{ J/kg}^\circ\text{C}$ , and rock grain density  $\rho_R = 2,600 \text{ kg/m}^3$ . Boundary conditions at the land surface are an atmospheric pressure of 1.013 bar and a temperature of 5 °C. Our model does not include an unsaturated zone so that, strictly speaking, these conditions apply at the elevation of the water table rather than at the land surface itself.

Prior to introducing CO<sub>2</sub> into the channel, an initial state is prepared that corresponds to a hydrostatic pressure profile for a geothermal gradient of 30 °C per km (Fig. 2), a typical value for continental crust. Injection is then initiated by applying CO<sub>2</sub> at the

bottom boundary of the channel at a pressure of 100 bar, which is considered a very modest overpressure in comparison to the equilibrated water pressure of 99.07

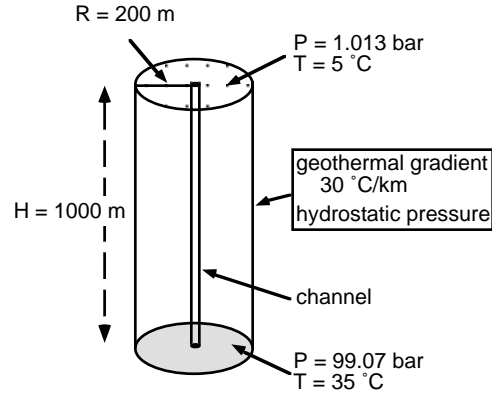


Figure 6. 2-D R-Z flow system.

bar at this elevation. Temperature at the bottom boundary is maintained at 35 °C, and pressure and temperature conditions at the outer (lateral) boundary are maintained constant at their initial values. At the present time no experimental data are available for constitutive properties of brine-CO<sub>2</sub> mixtures. We use Stone's (1970) three-phase water-oil-gas relative permeability formulation, assuming that water will be wetting and gaseous CO<sub>2</sub> non-wetting, with liquid CO<sub>2</sub> having intermediate wettability. Relative permeability parameters were chosen as in a typical three-phase flow problem involving water, soil gas, and a non-aqueous phase liquid (NAPL); more specifically, we use the same parameters as in the benzene-toluene flow problem presented as sample problem # 5 for TMVOC (Pruess and Battistelli, 2002). Capillary pressures were neglected.

For numerical simulation the system is discretized into 50 layers of 20 m thickness each. In the radial direction we use 27 grid blocks, starting with  $\Delta R = 1 \text{ m}$  in the center, and using larger  $\Delta R$  at larger distance from the channel.

#### 3.2 Results

The CO<sub>2</sub> entering the column partially dissolves in the aqueous phase, but most of it forms a separate liquid phase. Fig. 7 shows snapshots of the CO<sub>2</sub> plume at three different times. The CO<sub>2</sub> migrates primarily upward and also laterally outward from the high-permeability channel, reaching the land surface after 29.1 years. CO<sub>2</sub> rises as a liquid phase and flashes into gaseous CO<sub>2</sub> at a depth of approximately 630 m (Figs. 8-9), at thermodynamic conditions corresponding to the intersection of the profile of initial temperature and pressure conditions with the saturation line for CO<sub>2</sub> ( $T = 23.9 \text{ }^\circ\text{C}$ ,  $P = 62.8 \text{ bar}$ ; Fig. 2). The vaporization is partial and gives rise to evolution of a three-phase zone.

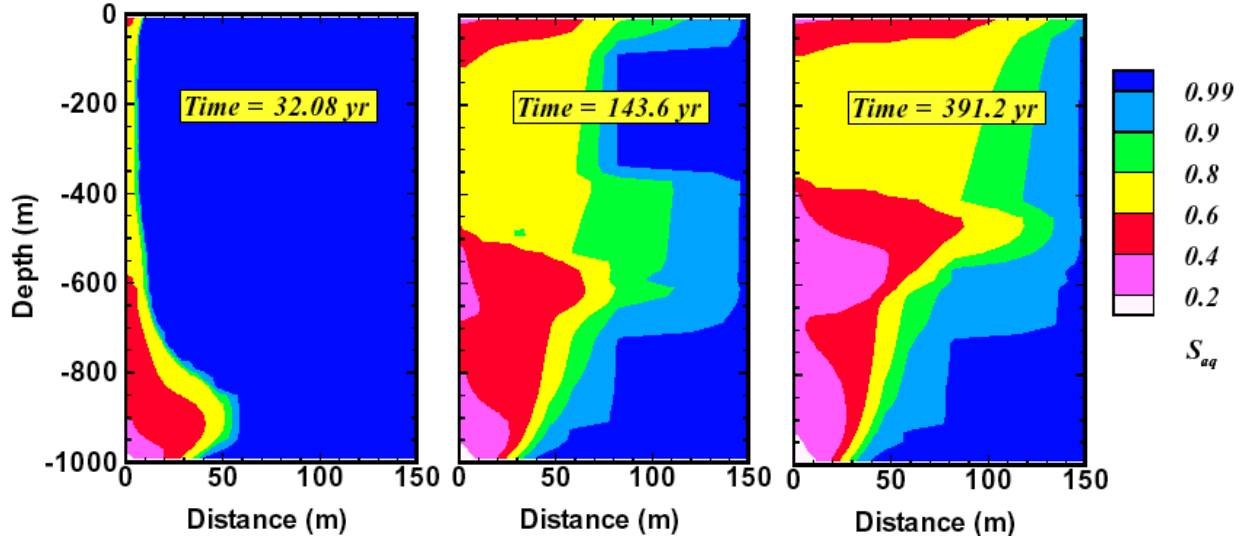


Figure 7. Snapshots of the CO<sub>2</sub> plume at three different times.

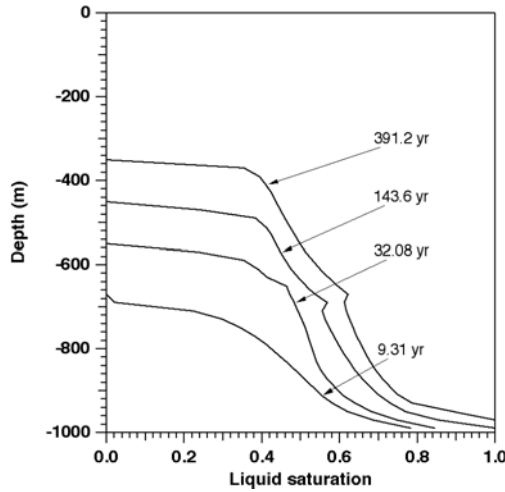


Figure 8. Advancement of the liquid CO<sub>2</sub> front in the center of the channel.

The processes of fluid flow, CO<sub>2</sub> dissolution, and phase change are accompanied by significant heat transfer effects (Figs. 10-12). At early time there is a modest temperature increase of approximately 3 °C in the two-phase (aqueous-liquid) zone, due to heat of dissolution of CO<sub>2</sub>. After a three-phase zone has formed, temperatures decline in the region of most intense CO<sub>2</sub> vaporization, near the top of the three-phase zone. The temperature decline from boiling of liquid CO<sub>2</sub> causes conductive cooling near the front. As the liquid front advances upward (Fig. 8) the three-phase zone becomes very broad (Fig. 9).

Our simulation stops after 391.2 years as freezing conditions are approached, because the fluid property treatment adopted here has no provisions to deal with phase change from liquid water to ice or solid hydrate phases.

The advancement of the liquid front slows down with time, while frontal temperatures become lower and always remain close to CO<sub>2</sub> saturation temperature at prevailing pressure (Fig. 11). This behavior can be understood from the linkage between pressures and temperatures in three-phase conditions (two-phase liquid-gas conditions for CO<sub>2</sub>). Fluid pressures never deviate much from the original hydrostatic values, and partial pressure of water vapor is small at the temperatures considered here. Where free-phase CO<sub>2</sub> is present, its partial pressure is close to the initial hydrostatic pressure at the same elevation. When liquid CO<sub>2</sub> enters a region with aqueous-gas conditions, it will be completely vaporized as long as the prevailing temperature remains above the saturation line,  $T > T_{\text{sat}}(P_{\text{CO}_2})$ . The vaporization process lowers temperatures and eventually gives rise to evolution of a liquid phase when the temperature drops to the saturated vapor temperature of CO<sub>2</sub> at prevailing pressure. Fig. 12 shows that the (T, P) profile tracks the CO<sub>2</sub> saturation line throughout the three-phase zone. At shallower depths, increasingly prolonged boiling is required to induce the larger temperature drops needed for advancement of the liquid CO<sub>2</sub> front. We can conclude that the advancement of the liquid front is entirely dominated by the thermal aspects of the problem.

Fluid mobilities are reduced in the three-phase zone from interference between the phases. This reduces flow rates in the vertical direction, slows the advancement of the liquid front (Fig. 11), and gives rise to lateral plume broadening and more dispersed discharge at the land surface (Fig. 13). Gas saturations increase to very large values due to decompression effects as the CO<sub>2</sub> approaches the land surface.

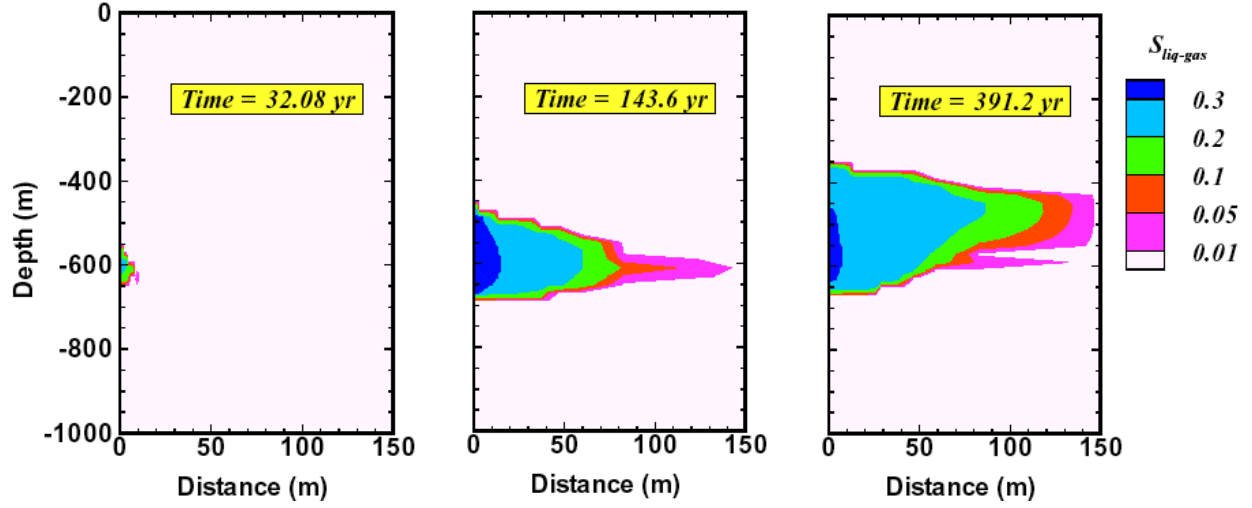


Figure 9. Extent of three-phase (aqueous-liquid-gas) zone at three different times. The quantity plotted is the geometric mean of liquid and gas saturations,  $S_{liq-gas} = \sqrt{S_{liq} \cdot S_{gas}}$ .

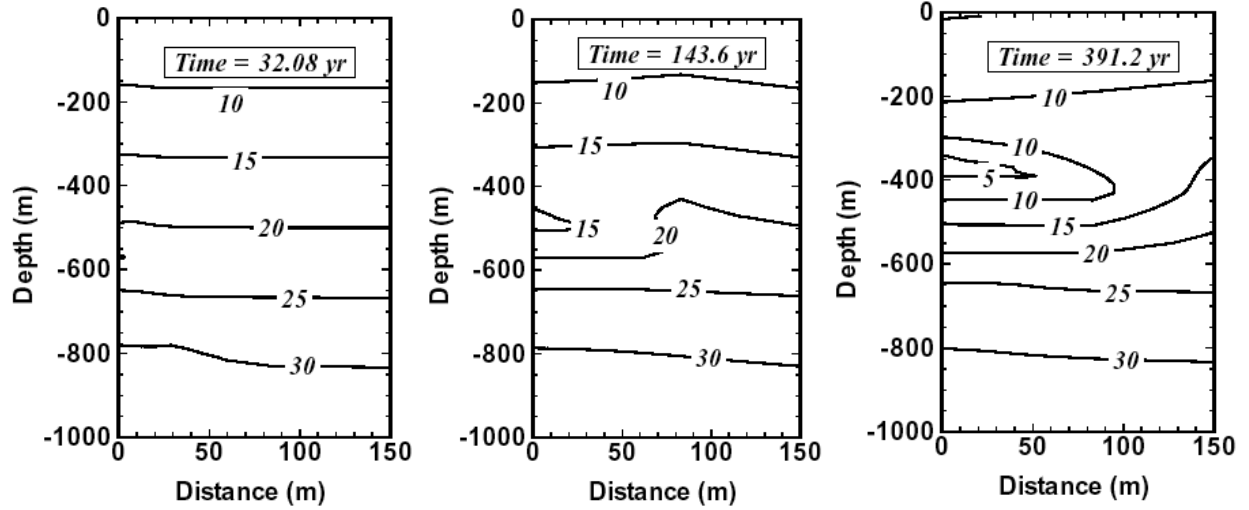


Figure 10. Temperature distributions ( $^{\circ}\text{C}$ ) at three different times.

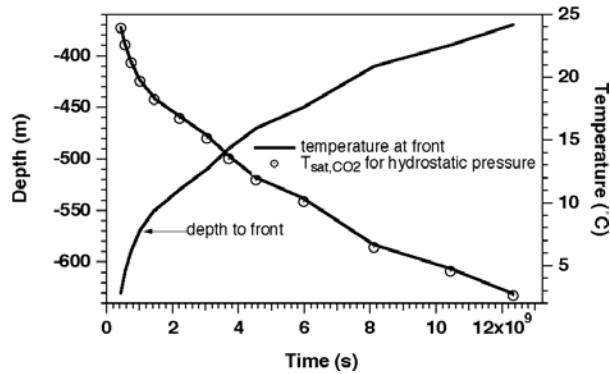


Figure 11. Advancement of liquid front, and frontal temperature, as function of time.

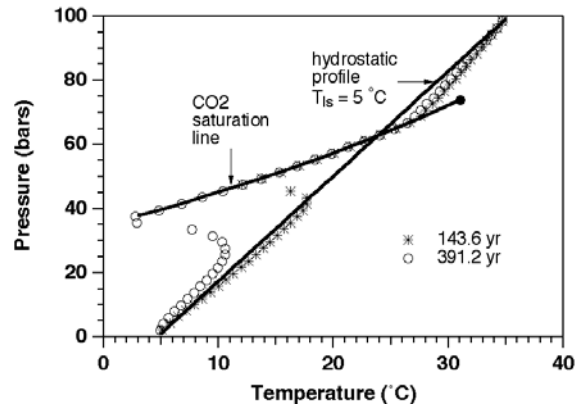


Figure 12. Temperature profiles in the center of the upflow channel at different times.

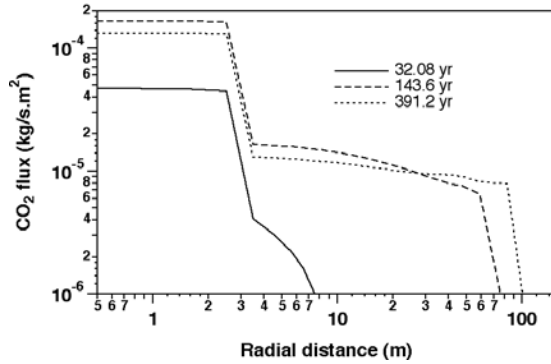


Figure 13. Profiles of CO<sub>2</sub> flux at the land surface at three different times.

#### 4. LARGER TEMPERATURE AT TOP BOUNDARY

It is of interest to investigate whether strong cooling effects can also occur when the initial temperature and pressure profile does not intersect the CO<sub>2</sub> saturation line. Accordingly, another simulation was performed for an average land surface temperature of  $T_{ls} = 15^\circ\text{C}$ , in which case CO<sub>2</sub> can pass from supercritical to gaseous conditions without a phase change (Fig. 2). Results for the evolution of temperature and pressure conditions in the central upflow channel are shown in Fig. 14. It is seen that in the region with supercritical pressures, temperatures rapidly decline towards a line that is an extension of the CO<sub>2</sub> saturation line. The cooling effects push the flow system towards the critical point, and subsequent evolution proceeds along the liquid-gas phase boundary, similar to what was seen in the  $T_{ls} = 5^\circ\text{C}$  case. The simulation was terminated after 1,214 years, at which time a minimum temperature of  $8.3^\circ\text{C}$  had been reached at 430 m depth.

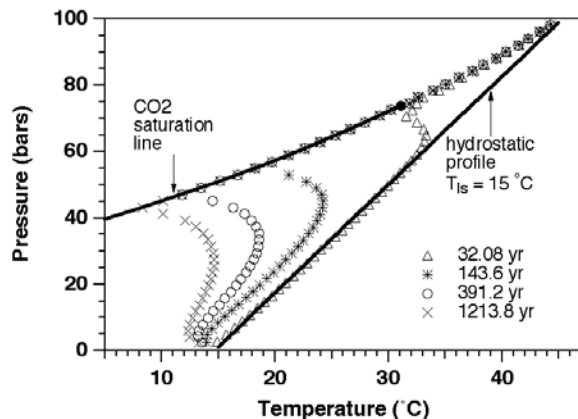


Figure 14. Temperature-pressure profiles in the center of the upflow channel for a case with land surface temperature of  $15^\circ\text{C}$  at different times.

#### 5. CONCLUDING REMARKS

Supercritical CO<sub>2</sub> escaping from a deep disposal reservoir may migrate along sub-vertical preferential pathways, such as fracture zones and faults, or old abandoned wells, and may eventually discharge at the land surface. CO<sub>2</sub> migration is affected by permeability structure and by multiphase fluid and heat transfer effects. Boiling of liquid CO<sub>2</sub> into gas consumes large amounts of latent heat and causes considerable cooling of the rock. A simulation for an average land surface temperature of  $T_{ls} = 5^\circ\text{C}$  was terminated after 391.2 years, when minimum temperatures had declined to below  $3^\circ\text{C}$ . At this point, the liquid CO<sub>2</sub> had advanced to a depth of 350 m. The results presented here suggest that temperatures would eventually drop below the freezing point of water if the flow process were run out longer. Solid water ice and hydrate phases would then form and reduce the permeability of the preferential CO<sub>2</sub> pathway, reducing gas fluxes and dispersing discharges at the land surface over a larger area.

In realistic groundwater systems another effect would come into play that could substantially reduce upflow of CO<sub>2</sub>. Regional groundwater flow may dissolve and remove significant amounts of CO<sub>2</sub>, reducing rates of upward migration of free-phase CO<sub>2</sub>. This effect requires a fully 3-D analysis and could not be represented in our axisymmetric model. Future work should also aim at a more realistic representation of geometric and hydrogeologic properties of potential pathways for CO<sub>2</sub> migration towards shallower strata, including features such as anisotropic, layered formations, and additional flow barriers such as shale layers that may divert CO<sub>2</sub> upflow sideways until another zone of caprock weakness is encountered. Model predictions are sensitive to constitutive properties for three-phase flows of water and liquid-gas mixtures of CO<sub>2</sub> for which no experimental data are available at present.

#### ACKNOWLEDGMENT

The author is grateful to Curt Oldenburg and George Moridis for their reviews and helpful suggestions. This work was supported by the Director, Office of Science, Office of Basic Energy Sciences of the U.S. Department of Energy under Contract No. DE-AC03-76SF00098.

#### REFERENCES

Adenekan, A.E., T.W. Patzek and K. Pruess. Modeling of Multiphase Transport of Multicomponent Organic Contaminants and Heat in the Subsurface: Numerical Model Formulation,

- Water Resour. Res.*, Vol. 29, No. 11, pp. 3727-3740, 1993.
- Altunin, V.V. *Thermophysical Properties of Carbon Dioxide*, Publishing House of Standards, 551 pp., Moscow, 1975 (in Russian).
- Battistelli, A., C. Calore and K. Pruess. The Simulator TOUGH2/EWASG for Modeling Geothermal Reservoirs with Brines and Non-Condensable Gas, *Geothermics*, Vol. 26, No. 4, pp. 437 - 464, 1997.
- Chivas, A.R., I. Barnes, W.C. Evans, J.E. Lupton and J.O. Stone. Liquid Carbon Dioxide of Magmatic Origin and its Role in Volcanic Eruptions, *Nature*, Vol. 326, No. 6113, pp. 587 - 589, 9 April 1987.
- Hitchon, B., W.D. Gunter, T. Gentzis and R.T. Bailey. Sedimentary Basins and Greenhouse Gases: A Serendipitous Association, *Energy Convers. Mgmt.*, Vol. 40, pp. 825 - 843, 1999.
- Holloway, S. and D. Savage. The Potential for Aquifer Disposal of Carbon Dioxide in the U.K., *Energy Convers. Mgmt.*, Vol. 34, No. 9 - 11, pp. 925 - 932, 1993.
- International Formulation Committee. *A Formulation of the Thermodynamic Properties of Ordinary Water Substance*, IFC Secretariat, Düsseldorf, Germany, 1967.
- Pruess, K., C. Oldenburg and G. Moridis. *TOUGH2 User's Guide, Version 2.0*, Lawrence Berkeley National Laboratory Report LBNL-43134, Berkeley, CA, November 1999.
- Pruess, K. and A. Battistelli. *TMVOC, a Numerical Simulator for Three-Phase Non-Isothermal Flows of Multicomponent Hydrocarbon Mixtures in Saturated-Unsaturated Heterogeneous Media*, Lawrence Berkeley National Laboratory Report LBNL-49375, Berkeley, CA, April 2002.
- Pruess, K. and J. García. Multiphase Flow Dynamics During CO<sub>2</sub> Injection into Saline Aquifers, *Environmental Geology*, Vol. 42, pp. 282 - 295, 2002.
- Pruess, K. Numerical Simulation of CO<sub>2</sub> Leakage from a Geologic Disposal Reservoir, Including Transitions from Super- to Sub-Critical Conditions, and Boiling of Liquid CO<sub>2</sub>, Lawrence Berkeley National Laboratory Report LBNL-52423, Berkeley, CA, March 2003.
- Sigurdsson, H., J.D. Devine, F.M. Tchoua, T.S. Presser, M.K.W. Pringle, and W.C. Evans. Origin of the Lethal Gas Burst from Lake Monoun, Cameroon, *J. Volcanol. Geotherm. Res.*, Vol. 31, pp. 1 - 16, 1987.
- Stone, H.L. Probability Model for Estimating Three-Phase Relative Permeability, *Trans. SPE of AIME*, 249, 214-218, 1970.
- Tazieff, H. Mechanism of the Nyos Carbon Dioxide Disaster and of so-called Phreatic Steam Eruptions, *J. Volcanol. Geotherm. Res.*, Vol. 391, pp. 109 - 116, 1991.
- Vargaftik, N.B. *Tables on the Thermophysical Properties of Liquids and Gases*, 2nd Ed., John Wiley & Sons, New York, NY, 1975.